Molecular Therapy
Oncolytics
Original Article

AMERICAN SOCIETY of GENE & CELL THERAPY

Inhibition of Cholesterol Esterification Enzyme Enhances the Potency of Human Chimeric Antigen Receptor T Cells against Pancreatic Carcinoma

Lei Zhao,[1,3] Yang Liu,[1] Fuya Zhao,[1] Ye Jin,[1] Jing Feng,[1] Rui Geng,[1] Jiayu Sun,[1] Liqing Kang,[2] Lei Yu,[2] and Yunwei Wei[1,3]

[1]Oncological and Laparoscopic Surgery Department, First Hospital of Harbin Medical University, Harbin, Heilongjiang Province 150001, China; [2]College of Chemistry and Molecular Engineering, East China Normal University, Shanghai 200241, China; [3]Translational Medicine Research and Cooperation Center of Northern China, Heilongjiang Academy of Medical Sciences, Heilongjiang 150001, China

This study aimed to assess the effectiveness of inhibiting cholesterol acyltransferase 1 (ACAT-1) in chimeric antigen receptor T (CAR-T) cells on potentiating the antitumor response against mesothelin (MSLN)-expressing pancreatic carcinoma (PC) cells. We engineered ACAT-1-inhibited CAR-T cells (CAR-T-1847 and CAR-T-1848) using the targeting MSLN CAR lentiviral vector and small interfering RNA (siRNA) targeting the conserved region of the *ACAT-1* gene, and characterized the efficacy of these modified CAR-T cells in terms of the cytotoxicity and cytokine release of both MSLN-positive and MSLN-negative PC cells using *in vitro* methods and *in vivo* mouse xenografts. The ACAT-1-inhibited CAR-T-1847 and CAR-T-1848 cells showed a higher cytotoxicity at effector-to-target cell (E:T) ratios of 8:1 and 10:1, respectively, and induced a higher secretion of proinflammatory cytokines interleukin-2 (IL-2) and interferon-gamma (IFNγ) *in vitro*. In addition, bioluminescence imaging of tumor xenografts of ACAT-1-inhibited targeting MSLN CAR-T cells in MSLN-positive PC mice *in vivo* showed significant tumor regression, which is consistent with the *in vitro* observations. Our findings demonstrate a novel immunotherapeutic strategy involving the transplantation of ACAT-1-inhibited targeting MSLN CAR-T cells and the feasibility of enhancing the antitumor potency of CAR-T through the novel strategy.

INTRODUCTION

Pancreatic carcinoma (PC) is an aggressive human digestive malignancy with a 5-year survival rate of less than 10%.[1] Although surgery is the primary treatment method, it is ineffective for more than half of PC patients with advanced unresectable or metastatic disease, according to the US Surveillance, Epidemiology, and End Results program data.[2] Moreover, treatment for PC chemotherapy with gemcitabine, gemcitabine plus nab-paclitaxel, or FOLFIRINOX has been shown to only slightly reduce the mortality rate (with median overall survival of ~5.9–11.1 months).[3,4] Hence there is an urgent need to develop novel and effective therapeutic strategies for PC.

Chimeric antigen receptor T (CAR-T) cells, which express engineered antigen receptors that recognize and eliminate cancer cells, have shown promise in the treatment of refractory and relapsed lymphocytic malignancies,[5,6] but have yet to show much efficacy against solid tumors. A major issue of current CAR-T cell technology is its relatively poor efficacy and safety due to the immune suppressive tumor microenvironment and off-target cytotoxicity issues.[7,8] Mesothelin (MSLN)-directed CAR-T cells have shown promise in the treatment of PC patients with peritoneal tumor metastasis without causing overt off-target cytotoxicity issues,[9,10] thus indicating the potential of developing efficacious CAR-T cell technology.

Currently, combination therapy and reprogramming the tumor microenvironment[9] have been the focus of most studies rather than enhancing the antitumor response of CAR-T cells. In our previous study, we demonstrated that inhibition of cholesterol acyltransferase 1 (ACAT-1) potentiated the antitumor response of CD19-directed CAR-T cells *in vitro*.[11] Acyl-coenzyme A (CoA):ACAT is the unique intracellular enzyme that converts the free cholesterol and fatty acid to cholesteryl esters (CEs), holding the pivotal status in maintaining intercellular homeostasis of lipids.[12,13] ACAT-1 is the primary enzyme for cholesterol metabolism in $CD8^+$ T cells,[14] which could induce proliferation and affect T cell function.[15] Therefore, we designed the present study to assess the efficacy of this strategy against PC tumors *in vitro* and *in vivo*. Specifically, we constructed genetically modified MSLN-directed CAR-T (targeting MSLN CAR-T) cells with small interfering RNA (siRNA) knockdown of the *ACAT-1* gene and determined their effect on PC cells *in vitro*. Then, we proceeded to confirm the observations found *in vitro* using *in vivo* mouse xenograft models. Our findings demonstrate the potential of modulating the metabolic processes of CAR-T cells as a viable strategy for treating solid tumors.

Received 18 November 2019; accepted 29 January 2020;
https://doi.org/10.1016/j.omto.2020.01.008.

Correspondence: Yunwei Wei, Oncological and Laparoscopic Surgery Department, First Hospital of Harbin Medical University, No. 23 Youzheng Street, NanGang District, Harbin City, Heilongjiang Province 150001, China.
E-mail: hydwyw@hrbmu.edu.cn

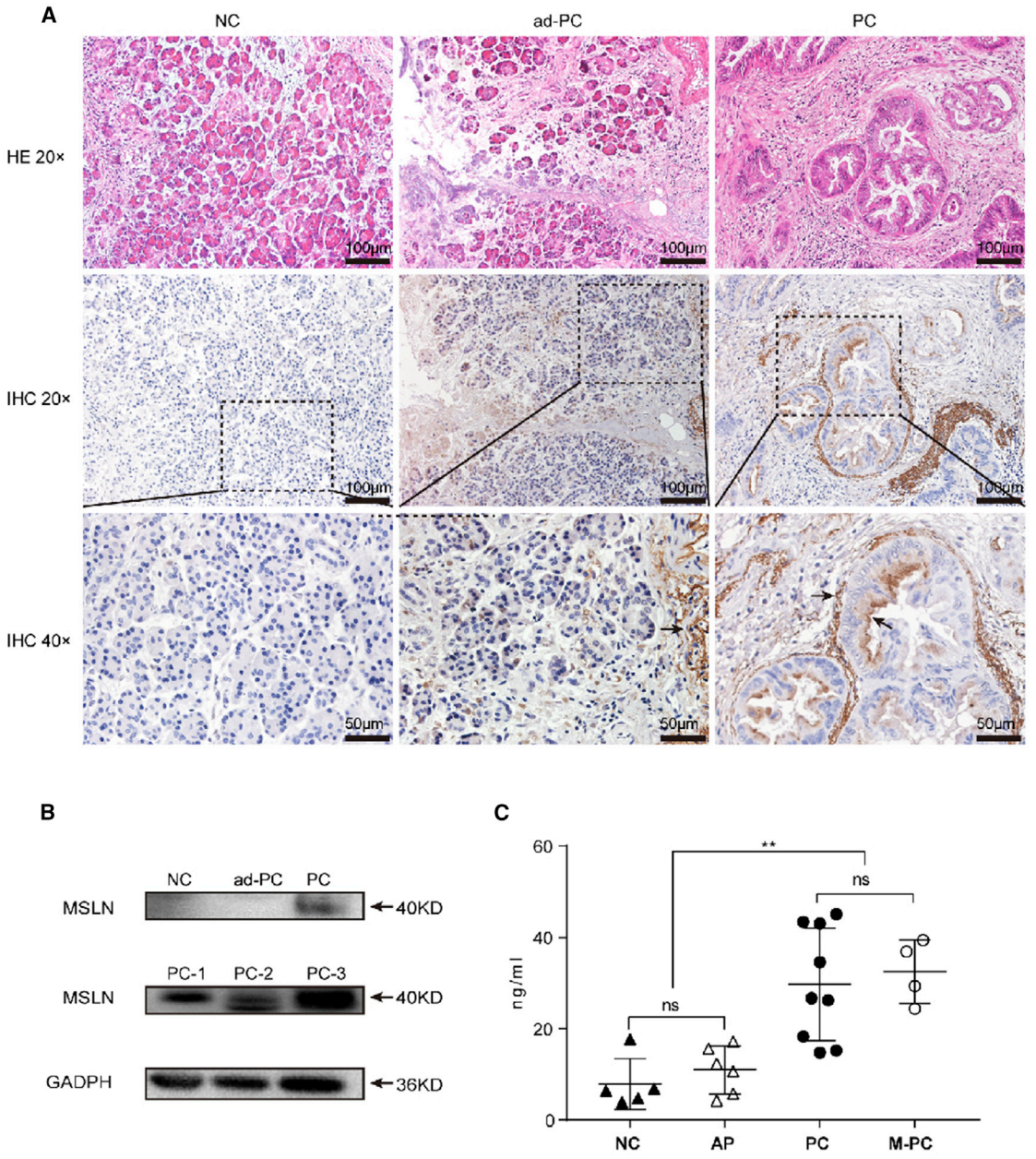

Figure 1. MSLN Overexpression in Human PC Patients

(A) Representative micrographs at ×20 and ×40 original magnification showing MSLN-positive PC cells. MSLN-positive tumor glands are indicated by the arrow. (B) MSLN expression in NC, ad-PC, and PC tissues. (C) ELISA profile showing the relative level of circulating soluble MSLN in patient serum samples. Each symbol represents a patient sample.

RESULTS

MSLN Is Overexpressed in PC Patient Serum and Tissue Samples

MSLN expression in the four groups of surgically resected specimens of human pancreatic adenocarcinoma was assessed using immunohistochemical staining. The surfaces of tumor glands, but not of normal glands, in normal (negative control [NC]) and adjacent PC (ad-PC) were MSLN positive (Figure 1A). Our observations were consistent with previous reports of MSLN expression in pancreatic adenocarcinoma.[16] Electrophoresis and western blot analysis revealed that the PC tissues were MSLN positive, whereas the NC and ad-PC tissues were MSLN negative (Figure 1B). In addition, enzyme-linked

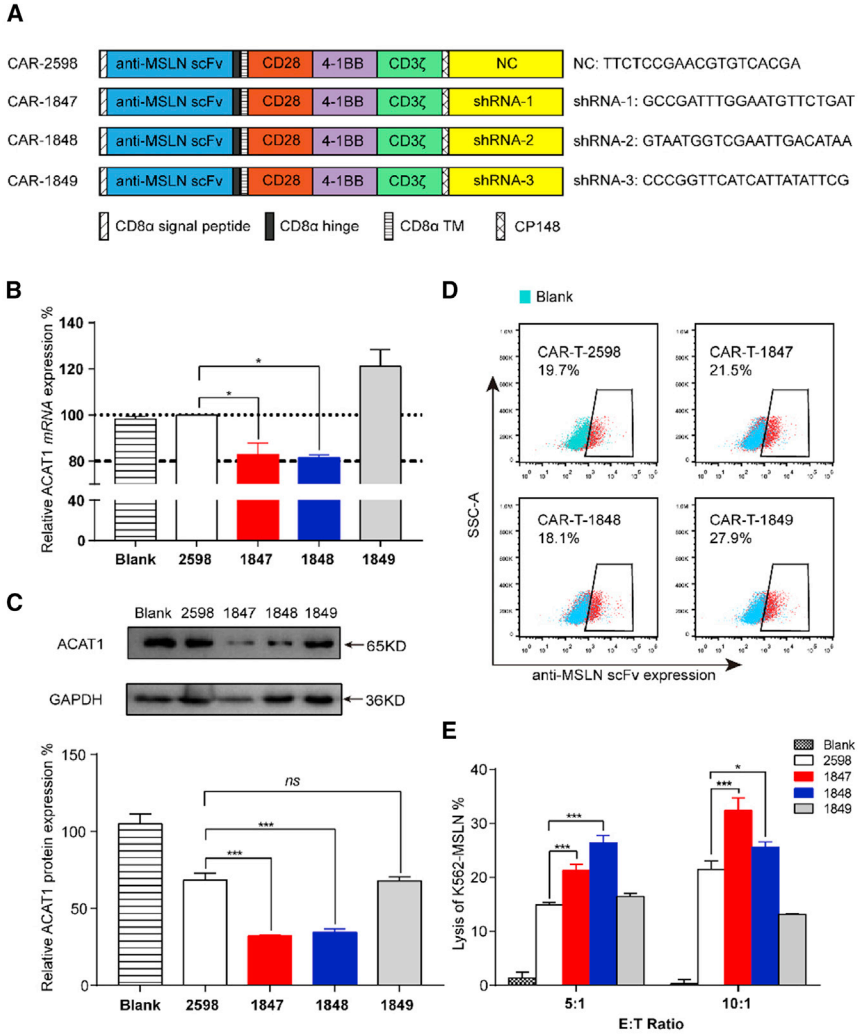

Figure 2. Generation and Characterization of *ACAT-1*-Inhibited Anti-MLSN CAR-T Cells

(A) Schematic representation of MSLN-targeted constructs with a *CD28* and *4-1BB* costimulatory domain, a *CD3ζ* domain, and an *ACAT-1* DNA suppression sequence. (B) Quantitative real-time RT-PCR profile showing *ACAT-1* mRNA levels in CAR-T-1847, CAR-T-1848, and CAR-T-2598 cells. (C) Western blot image showing the ACAT-1 protein level in CAR-T-1847, CAR-T-1848, and CAR-T-2598 cells. (D) Flow cytometry profile showing the transduction efficiencies. (E) LDH profile of different anti-MLSN CAR-T constructs.

immunosorbent assay (ELISA) showed that the levels of circulating soluble MSLN in PC (29.70 ± 11.58 ng/mL) and PC with metastasis (M-PC) (32.50 ± 5.98 ng/mL) were also significantly higher than those in NC (7.91 ± 4.99 ng/mL) and acute pancreatitis (AP) (10.97 ± 4.74 ng/mL) ($p < 0.01$; Figure 1C). Thus, these results indicate that PC patients who have MSLN overexpressed in tissues or the circulation are potential candidates for CAR-T immunotherapy.

Generation and Characterization of Targeting MSLN CAR-T Cells with *ACAT-1* Inhibition

We used targeting MSLN HN1 single-chain variable fragment (*scFv*) CARs, which have been shown to be safe and have a high efficacy in clinical trials.[17] We created a series of targeting MSLN scFv-based CARs comprising a *CD3ζ* domain, a *CD28* and *4-1BB* costimulatory intracellular domain, and an anti-ACAT-1 tandem DNA sequence (Figure 2A). CAR-2598 without having the anti-ACAT-1 tandem DNA sequence was used as the negative control (NC). The third-generation lentiviral-vector technique involving the cloning of cDNA sequences with the *EF-1α* promoter,[18] which was validated in our previous research,[11] was used to assess CAR-T expression in this study. An approximately 20% reduction in the relative *ACAT-1* mRNA level in CAR-T-1847 (82.97% ± 3.39%) and CAR-T-1848 (81.44% ± 0.87%) cells was observed, compared with that in CAR-T-2598 cells ($p < 0.05$; Figure 2B). In addition, the ACAT-1 protein levels in CAR-T-1847 and CAR-T-1848 cells were also significantly lower than that in CAR-T-2598 cells ($p < 0.05$; Figure 2C). A medium transduction efficiency level (18.1%–27.9%) of T cells with the CAR-lentiviral vector was observed (Figure 2D). The lactate dehydrogenase (LDH) release from K562 and MSLN-K562 cells at an effector-to-target cell (E:T) ratio of 10:1 was determined to assess the antitumor potential of CAR-T cells. All engineered targeting MSLN CAR-T cells showed a high cytotoxicity against MSLN-K562 cells, but not MSLN-negative K562 parental cells, indicating their efficiency and specificity. Furthermore, CAR-T-1847 ($p < 0.001$) and CAR-T-1848 ($p < 0.05$) cells exhibited a higher cytotoxicity than CAR-T-2598 cells against MSLN-positive K562 cells (Figure 2E).

ACAT-1 Inhibition Decreases CAR Transduction Efficiency

Because *Acat1*^{CKO} mice have been found to produce more cytotoxic interferon-gamma$^+$CD8$^+$ (IFNγ$^+$CD8$^+$) and tumor necrosis factor-alpha$^+$CD8$^+$ (TNF-α$^+$CD8$^+$) T cells,[14] we evaluated the distribution of the CD8$^+$ subtypes in ACAT-1-inhibited CAR-T cells. The transduction efficiencies of ACAT-1-inhibited CAR-T cells were assessed for six different cases (Table S1). The transduction efficiencies of CAR-T-1847 and CAR-T-1848 cells were significantly lower than that of CAR-T-2598 cells ($p < 0.001$; Figures 3A and 3B). There were no significant differences in the percentages of CD8$^+$ CAR-T, IFNγ$^+$CD8$^+$ CAR-T, and TNF-α$^+$CD8$^+$ CAR-T cells among all three groups ($p > 0.05$; Figures 3C–3H), indicating that a reduction in the CAR transduction efficiencies due to ACAT-1 inhibition did not affect the proportion of the CD8$^+$ CAR-T subtypes.

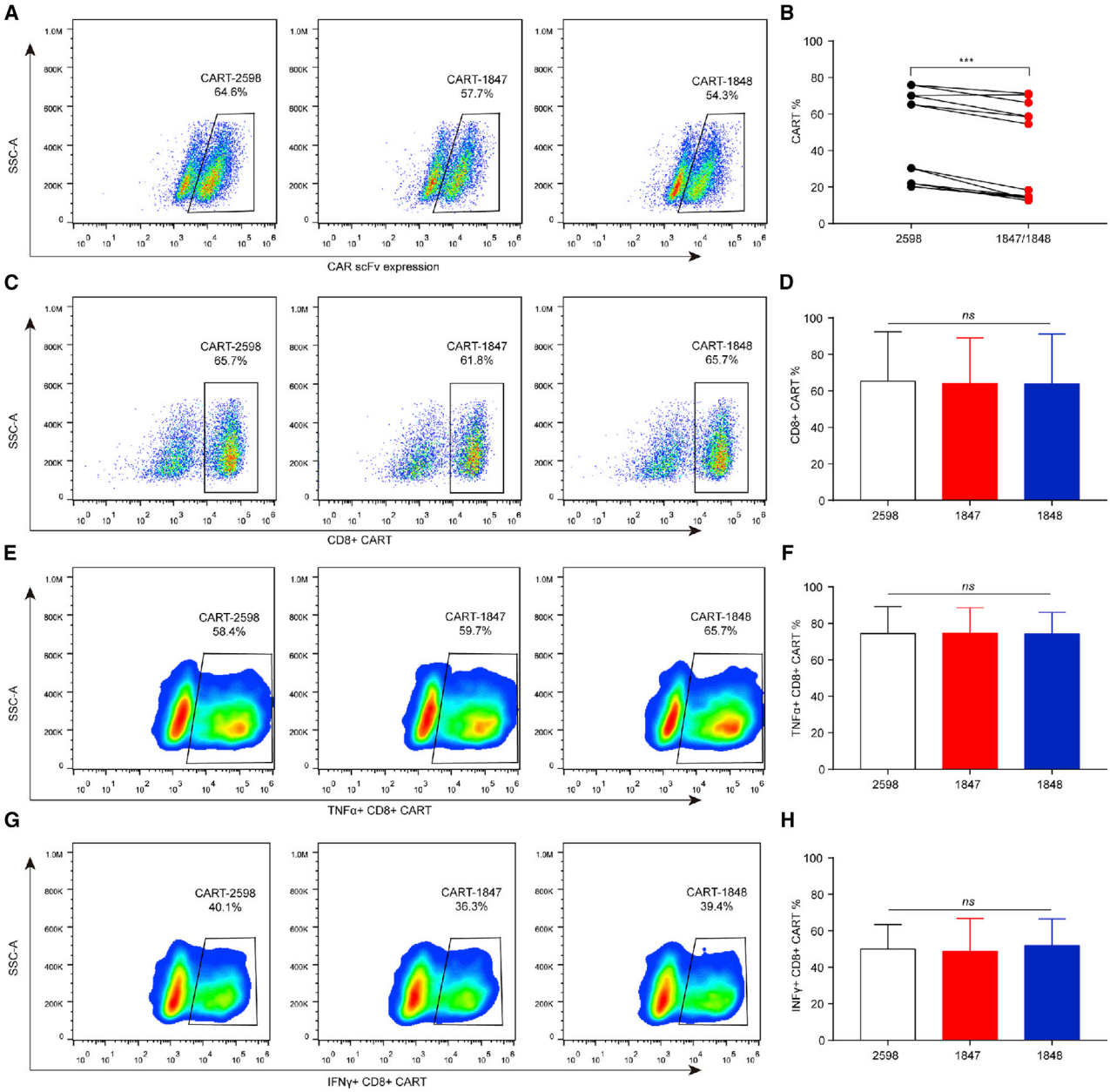

Figure 3. The Phenotype of Anti-MLSN CAR-T Cells

(A–H) Flow cytometry profile showing the (A and B) transduction efficiencies of CAR-T cells and the (C–H) percentage distribution of $CD8^+$, $IFN\gamma^+CD8^+$, and $TNF\text{-}\alpha^+$ $CD8^+$ targeting MSLN CAR-T cells. Representative results from one of six patients are shown. (A and B) The transduction efficiencies of CAR-T-1847 and CAR-T-1848 cells were significantly lower than that of CAR-T-2598 cells ($P < 0.001$). (C–H) There were no significant differences in the percentages of $CD8^+$ CAR-T, $IFN\gamma^+CD8^+$ CAR-T, and $TNF\alpha^+CD8^+$ CAR-T cells among all three groups ($P > 0.05$).

ACAT-1 Inhibition Potentiates the Antitumor Function of Human Targeting MSLN CAR-T Cells

To further test whether inhibiting *ACAT-1* in targeting MSLN CAR-T cells could enhance their cytotoxicity toward MSLN-positive targets, we performed a standard LDH release assay using *in vitro* cocultures of MSLN-K562 cells and different T cells, and then normalized the results with respect to the transduction efficiencies of CAR-T-2598 and CAR-T 1847/1848 cells. There was no significant difference among groups at an E:T ratio of 5:1 ($p > 0.05$; Figure 4A), but CAR-T-1847 cells showed a higher cytotoxic effect at E:T ratios of 8:1 ($p < 0.001$; Figure 4B) and 10:1 ($p < 0.01$; Figure 4C). In addition, CAR-T-1848 cells showed a higher

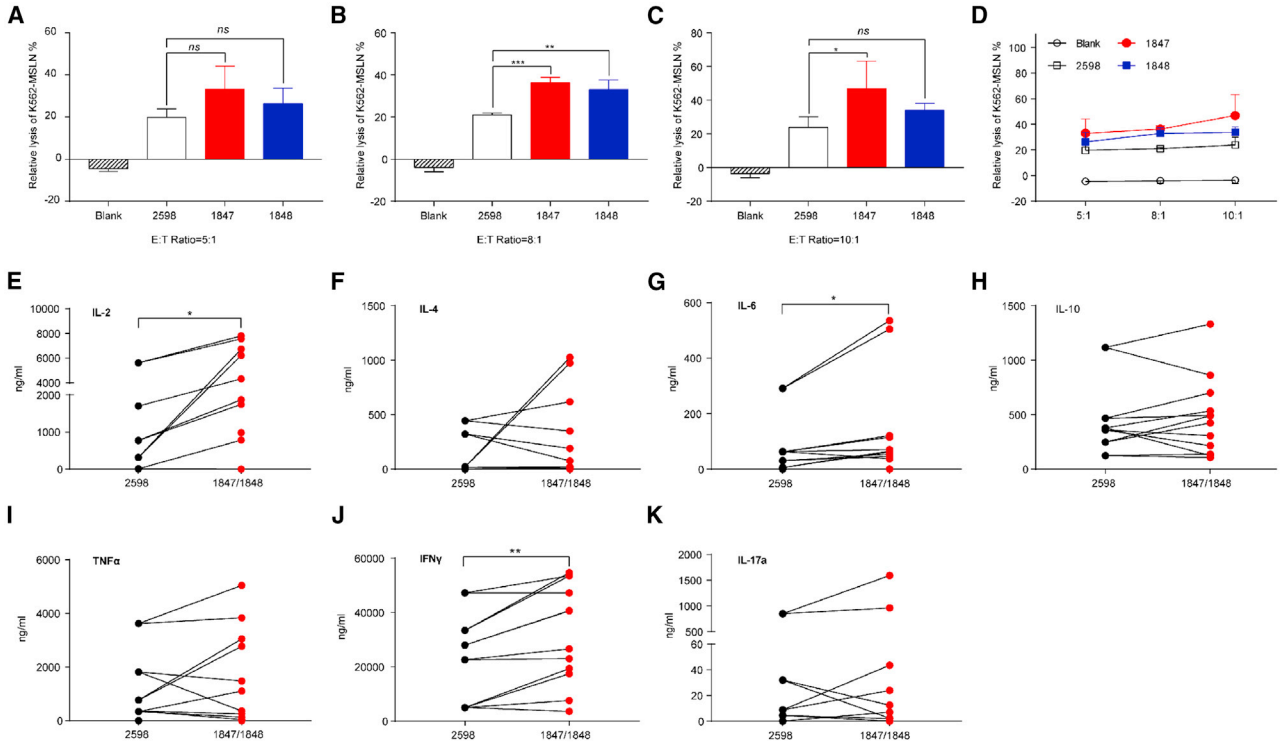

Figure 4. ACAT-1 Inhibition Enhanced the Targeting MSLN CAR-T Antitumor Function

Targeting MSLN CAR-T cells were cocultured with target cells at different E:T ratios for 18 h. (A–C) Cell lysis of cocultures was assessed with a standard LDH release assay at E:T ratios of (A) 5:1, (B) 8:1, and (C) 10:1. (D) Profile showing the dose-dependent lysis of MSLN-K562 cells by targeting MSLN CAR-T cells. (E–K) Profiles showing the results of the cytokine release assay. (B and C) CAR-T-1847 cells showed a higher cytotoxic effect at E:T ratios of 8:1 and 10:1. (B) CAR-T-1848 cells also showed a higher cytotoxic effect at an E:T ratio of 8:1. (D) Dose-dependent lysis of MSLN-K562 cells by targeting MSLN CAR-T cells was bserved. (E and J) CAR-T-1847 and CAR-T-1848 cells induced higher levels of IL-2 ($P < 0.05$) and IFNγ ($P < 0.01$) production compared to that by CAR-T-2598 cells.

cytotoxic effect at an E:T ratio of 8:1 ($p < 0.01$; Figure 4B). Dose-dependent lysis of MSLN-K562 cells by targeting MSLN CAR-T cells was observed (Figure 4D). The release of cytokines from T helper 1 (Th1; e.g., IFNγ, TNF-α, and interleukin-2 [IL-2]) and T helper 2 (Th2; e.g., IL-4, IL-6, IL-10, and IL-17a) cytokines by CAR-T cells was assessed using coculture assays at an E:T ratio of 8:1. We found that CAR-T-1847 and CAR-T-1848 cells induced higher levels of IL-2 ($p < 0.05$) and IFNγ ($p < 0.01$) production compared with that by CAR-T-2598 cells (Figures 4E and 4J). In addition, CAR-T-1847 and CAR-T-1848 cells induced significantly higher IL-6 ($p < 0.05$) production than CAR-T-2598 cells (Figure 4G). However, there was no significant difference in the levels of IL-4, IL-10, TNF-α, and IL-17a released ($p > 0.05$; Figures 4F, 4H, 4I, and 4K), and there was negligible cytokine release in all MSLN-negative target groups (Figure S1). ACAT-1 inhibition in targeting MSLN CAR-T cells enhanced cytotoxicity and induced Th1 cytokine (IL-2 and IFNγ) secretion.

ACAT-1 Inhibition Enhanced the Antitumor Efficacy of Targeting MSLN CAR-T Cells *In Vivo*

Next, we established xenograft mouse models by transplanting MSLN-BxPC-3-Luci PC cells into the flanks of nonobese diabetic-severe combined immunodeficiency (SCID) gamma (NSG) mice and observed rapid MSLN-BxPC-3-Luci cell proliferation and constitutive MSLN expression (Figure S2). When the tumor volume reached approximately 500 mm^3 (around the 12^{th} day after transplantation), the mice were randomly divided into four groups and subjected to three intratumoral injections of 1×10^7 CAR-T-2598, CAR-T-1847, and CAR-T-1848 cells (50%–70% transgene-positive) and an equivalent volume of phosphate-buffered saline (Blank group), respectively, every 4–5 days (Figure 5A). The fastest tumor growth was observed in the NC group at around 2 weeks after targeting MSLN CAR-T cell administration. Bioluminescence imaging showed that sustained tumor regression was observed for CAR-T-1847 cells compared with the Blank and CAR-T-2598 groups at day 33 ($p < 0.05$; Figures 5B–5D). In addition, the CAR-T-1847 group showed a significantly reduced tumor volume compared with that of the CAR-T-2598 group (120.29 ± 98.04 versus 379.18 ± 63.19 mm^3; $p < 0.05$; Figures 5E and 5F). However, there was no significant difference in the animal weight or CAR-T cell infiltration among groups (Figure S3). Taken together, *ACAT-1* inhibition increased the potency of targeting MSLN CAR-T cells' cytotoxicity, thereby inducing MSLN-positive PC tumor regression *in vivo*.

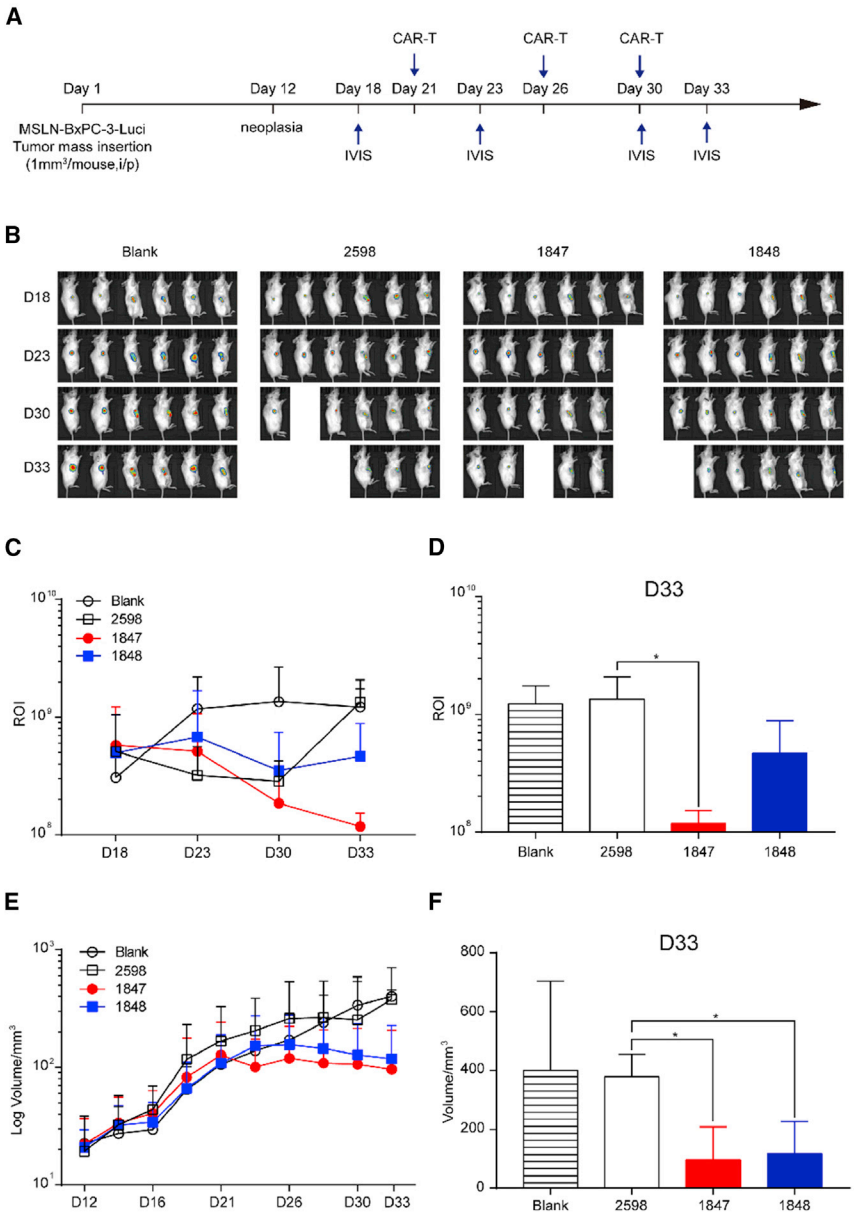

Figure 5. *ACAT-1* Inhibition Increased the Targeting MSLN CAR-T Cell Potency against MSLN-BxPC-3-Luci Xenografts *In Vivo*

(A and B) Tumor bioluminescence images of mice transplanted with MSLN-BxPC-3-Luci tumor cells at the indicated time points. (C and D) Comparison of the tumor bioluminescence intensities between the CAR-T and control groups. Bioluminescence imaging showed that sustained tumor regression was observed for CAR-T-1847 cells compared to the Blank and CAR-T-2598 groups at day 33 ($P < 0.05$). (E and F) Comparison of the tumor volume between the CAR-T and control groups. CAR-T-1847 group showed a significantly reduced tumor volume compared to that of the CAR-T-2598 group (120.29 ± 98.04 mm^3 vs. 379.18 ± 63.19 mm^3; $P < 0.05$).

DISCUSSION

PC is one of the most lethal cancers worldwide. CAR-T immune therapy is one of the most promising anti-PC therapy strategies (technologies) reported. To reach the clinical safety and efficacy, the ideal CAR-T cells should be able to specifically recognize and target tumor cells, proliferate, and persist against immunosuppressive cells and factors in the tumor microenvironment.[19]

"Off-tumor, on target" is one of the most important safety issues for CAR-T treating the solid tumor. MSLN, a cell-surface tumor-associated antigen implicated in tumor invasion and proliferation, is highly expressed in PC and other cancers.[17] In this study, we confirmed that MSLN was overexpressed in both the tumors and sera of PC patients with and without metastasis, and showed low expression in normal pancreatic tissue. Previous studies have demonstrated the safety and modest efficacy of MSLN antibodies and vaccines in treating solid tumors,[20] indicating that MSLN is a potential target in PC CAR-T therapy. In fact, MSLN is a common CAR target in PC clinical trials. However, considering that fewer than 50% of PC patients showed stable disease,[10,21] further improvements in targeting MSLN CAR-T cells are necessary to increase the success rate of CAR-T cell therapy.

The modest response of PC tumors to CAR-T immunotherapy may be caused by the influence of the varied immunosuppressive cells and factors present in the tumor microenvironment. Hence the common strategies to enhance the efficacy of CAR-T cells reported include enhancing chemokine receptor[22] and combinatorial antigen receptor[23] expression, and/or blocking checkpoint receptor expression[24] on the T cell membrane. However, these strategies did not show much efficacy against PC tumors, and the already crowded CAR-T cell membrane by basic cell components limits the extent of modifications that can be performed without compromising the membrane integrity. Thus, we decided to use a different strategy to target the metabolic processes of CAR-T cells instead, which has been not been explored previously. Cellular lipid metabolic processes play vital roles in directing T cell proliferation and differentiation. Changes in fatty acid and cholesterol content have been found to induce proliferation and differentiation of effector T cells,[15] affect T cell function,[25] and promote T cell receptor phosphorylation.[26] Moreover, inhibiting *ACAT-1*, which converts free cholesterol and fatty acids to CEs, thereby increasing the cholesterol level in the

plasma membrane, has been shown to potentiate the antitumor response of $CD8^+$ T cells after activation.[14] In contrast, *ACAT-1*^{CKO} $CD8^+$ T cell proliferation and survival were also promoted.[14] In this study, we designed and engineered *ACAT-1* siRNA knockdown in targeting MSLN CAR-T cells and determined their potency against PC tumor cells. We found that *ACAT-1* inhibition significantly enhanced the cytotoxicity of targeting MSLN CAR-T cells and increased the secretion of the cytokines IFN-γ and IL-2 against MSLN-positive tumor cells. Of note, the tumor cell cytotoxicity was positively correlated with the E:T ratio. Moreover, consistent with our findings *in vitro*, we also observed an enhanced antitumor effect of targeting MSLN CAR-T cells with inhibited *ACAT-1* in MSLN-positive PC xenograft tumor models. Thus, our study successfully validated the strategy of inhibiting an enzyme involved in cholesterol metabolism, *ACAT-1*, to potentiate the action of human CAR-T against PC tumors.

During the construction of the basic targeting MSLN CAR-T complex with *ACAT-1* siRNA knockdown, we identified the conserved *ACAT-1* sequence by sequence alignment with three isoforms of *ACAT-1* (*SOAT-1*) mRNA (NM_003101.5, NM_001252512.1, and NM_003101.6) and used that for designing *ACAT-1* siRNA according to Tuschl's pattern using the following five criteria: GC percentage of 30%–52%, exclusion of a run of four or more T or A in a row, exclusion of a run of four or more Gs in a row, inclusion of fewer than seven consecutive GC in a row, and siRNAs should end with NN. The *ACAT-1* siRNA reduced the *ACAT-1* mRNA level by only approximately 20%. This low knockdown efficiency could be due to an inherently low *ACAT-1* expression, susceptibility to interference from other proteins in the CAR-T cells during testing, and the presence of pre-existing *ACAT-1* mRNA in T cells. Nonetheless, partial ACAT-1 knockdown appeared to suffice because a significantly reduced ACAT-1 protein level was observed in targeting MSLN CAR-T cells with *ACAT-1* siRNA. Moreover, *ACAT-1* inhibition was accompanied by reduced CAR transduction efficiencies. Hence more effective *ACAT-1* knockdown may instead further decrease the CAR transduction efficiencies. Despite the reduced CAR transduction efficiencies due to *ACAT-1* knockdown, there was no difference in the proportion of cytotoxic $CD8^+$ CAR-T, $IFN\gamma^+CD8^+$ CAR-T, and $TNF\text{-}\alpha^+CD8^+$ CAR-T subtypes. However, we observed changes in the distribution of the $CD8^+$ subtypes in our previous study,[11] which may be because of the different statistical methods used.

One of the limitations of this study was the low *ACAT-1* knockdown efficiency. The main reason that we did not knock out *ACAT-1* is that we considered the physiological function of ACAT-1. However, the most suitable *ACAT-1* knockdown efficiency should be discussed in our further research. Another limitation of this study was that we did not study the relationship between the *ACAT-1* knockdown efficiency and the transduction efficiencies, as well as the financial constraints that also prevented us from expanding the scope of our study to include the investigation of central genes that regulate cholesterol metabolism. These would be further discussed in our next study. Nonetheless, this strategy of *ACAT-1* inhibition can potentially be combined with other immunotherapeutic approaches involving the PD-1 antibody to further boost the antitumor efficacy of CAR-T cells. Future studies using animal models should be performed to validate this combination immunotherapy strategy.

In summary, *ACAT-1* inhibition increased the secretion of the proinflammatory cytokines IFN-γ and IL-2, thereby enhancing the antitumor response of targeting MSLN CAR-T cells against PC tumors in mice. In addition, our findings suggest the potential application of modified CAR-T cells for PC immunotherapy and possibly for the treatment of solid malignancies in general. Furthermore, our results expand the spectrum of possible modifications to CAR-T cells and might open a new field and provide a novel strategy to improve CART anti-tumor efficacy without influencing therapeutic safety.

MATERIALS AND METHODS

Patient Sample Collection and Processing

Peripheral blood from healthy donors (n = 5), AP patients (n = 6), PC patients (n = 9; diagnosed by enhanced computed tomography scanning or pathology), and metastatic PC patients (n = 4) was collected. Immediately after collection, the serum samples were obtained by centrifugation at 400 × *g* for 5 min (Table S2) and were stored at −80°C for subsequent ELISAs.

Surgically resected tumor specimens were obtained from PC patients who underwent surgery without neoadjuvant therapy. The resected tumor, adjacent mucosa, and normal pancreas were immediately immersed in ice-cold complete medium (Dulbecco's modified Eagle's medium containing 10% fetal bovine serum and 1% penicillin/streptomycin; GIBCO, Thermo Fisher Scientific, USA) before either flash freezing for western blot assays or fixing with formalin for immunohistochemistry and immunofluorescence assays.

All experiments involving the use of human specimens were approved by the Ethics Committee of First Hospital of Harbin Medical University and were conducted according to the principles outlined in the Declaration of Helsinki.

Animal Handling, Grouping, and Tumor Imaging

Thirty female NSG mice, aged 5–7 weeks (Jiangsu Jizhi Yaokang Biological Technology, China), were used to establish the PC animal models. All procedures were performed with the approval from the Institutional Animal Care and Use Committee. Mice were anesthetized using inhaled isoflurane and oxygen, and were injected with the analgesic bupivacaine. Next, MSLN-BxPC-3-Luci tumor cell masses (1 mm^3) were transplanted into the flank of the mice, and these tumor-bearing mice were randomly divided into four groups (one NC group and three treatment groups). Each treatment group was treated with 1×10^7 CAR-T cells (CAR-T 2598, CAR-T 1847, or CAR-T 1848) in 150 μL of serum-free medium, respectively, via direct intratumoral injection when the tumors reached approximately 500 mm^3. A 150-μL sample of serum-free medium was injected directly into the flank of the tumor-bearing mice in the Blank group.

In all four groups, the tumor size was measured every 2–4 days, and the tumor volume was calculated as V (mm^3) = $\pi/6 \times W^2 \times L$, where W and L are the width and the length of the tumor, respectively.

Bioluminescence imaging of the mouse tumors using the luciferase reporter assay, wherein the mice were intraperitoneally injected with a single dose of 150 mg/kg D-luciferin (Shanghai Yisheng Bio-Technology, China), was performed weekly using the IVIS Lumina IIIIVIS Imaging System (PerkinElmer, Waltham, MA, USA), and image analysis was carried out using Living Image 2.60 software (PerkinElmer, USA).

Cell Lines

The cell lines myeloid leukemia K562 and human pancreatic adenocarcinoma BxPC-3 were obtained from and authenticated by short tandem repeat (STR) profiling using the human STR profiling cell authentication service at American Type Culture Collection (Manassas, VA, USA). Red fluorescent protein (RFP)-tagged MSLN was lentivirally transduced into K562 cells to produce the MSLN-K562-RFP cell line. The MSLN-BxPC-3-Luci cell line was generated using BxPC-3 cells transduced with a lentiviral vector encoding the MSLN and luciferase reporter genes. K562, MSLN-K562-RFP, BxPC-3, and MSLN-BxPC-3-Luci cells expressing MSLN were identified by flow cytometry, western blotting, and quantitative reverse transcription-polymerase chain reaction (RT-PCR) (Figure S4).

Histology and Immunostaining

All human and mouse tissue sections (5 mm thick) were fixed with 4% paraformaldehyde (Sangon Biotech, Shanghai, China) and then embedded with paraffin (Leica, Germany) before staining with hematoxylin and eosin or were treated with standard antigen-retrieval methods for immunohistochemistry and immunofluorescence experiments. The primary antibodies MSLN (1:200; ab133489), CD3 (1:250; ab11089), and CD8 (1:100; ab4055) (all from Abcam, USA), as well as the secondary antibody Alexa Fluor 488 AffiniPure goat anti-rabbit IgG (111-545-144; Jackson ImmunoResearch, West Grove, PA, USA), were used for the immunohistochemistry and immunofluorescence assays.[10,27]

Western Blotting

Proteins from cell lysates were separated by 8% sodium dodecyl sulfate gel electrophoresis, transferred onto nitrocellulose membranes, and then probed with the MLSN mAb primary antibody (1:500; ab133489; Abcam, USA) for 24 h at 4°C. This procedure was followed by incubation with horseradish peroxidase-conjugated AffiniPure goat anti-mouse IgG secondary antibody (115-035-008; Jackson ImmunoResearch) for 1 h at room temperature.

ELISA

The level of soluble MSLN protein in human serum was determined using an ELISA kit (ab216168; Abcam, USA), according to the manufacturer's instructions. The MSLN protein levels were determined at 450 nm using a microplate reader (Thermo Fisher Scientific, USA).

Lentivirus Construction and Transduction

Targeting MSLN CAR consists of an MSLN single-chain antibody, a *CD8α* transmembrane hinge region, a *CD28* and *CD137* costimulatory domain, and a *CD3ζ* domain. CAR-T-1847, CAR-T-1848, and CAR-T-1849 cells were infected with the lentivirus containing *ACAT-1* siRNA, which was synthesized and amplified based on available sequencing information,[28] as well as data from our primary research.[11] The targeting MSLN CAR lentiviral vector was a gift from Prof. Lei Yu (East China Normal University, China). Peripheral blood mononuclear cells were isolated by Ficoll density gradient centrifugation. $CD3^+$ T cells were sorted with magnetic beads (130-050-101; Miltenyi Biotec, Germany) and were then transduced with targeting MSLN CAR lentivirus for 6 h. CAR-T cells were expanded and handled as described previously.[11]

Quantitative Real-Time RT-PCR

Total RNA was isolated with TRIzol (15596-026; Invitrogen, Thermo Fisher Scientific, USA) and reverse transcribed using a High-Capacity cDNA Reverse Transcription Kit (R223-01; Vazyme, Guangzhou, China). The primer sequences used for RT-PCR are as follows: MSLN, forward 5′-TAAAGCATAAACTGGATGA-3′ and reverse 5′-ATCTTGAGGAAGAGGTAG-3′; *ACAT-1*, forward 5′-CCTTGG CTGTTTGCTTGAGCTT-3′ and reverse 5′-CATCAGAACATTC CAAATCGGCTT-3′. Quantitative real-time PCR was performed using the Applied Biosystems 7500 Real-Time PCR System (Serial Number: 4489165) and the SYBR Green dye (Thermo Fisher Scientific, USA). The PCR conditions used were 95°C for 5 min and 40 cycles of 95°C for 10 s and 60°C for 34 s. Gene expression was normalized to internal housekeeping genes.

LDH Cytotoxicity Assay

Cocultures of different ratios of target cells and CAR-T cells were seeded in 96-well plates and were incubated in 100 mL of medium (RPMI 1640 medium containing 10% fetal bovine serum, 100 U/mL penicillin, 100 mg/mL streptomycin, and 1% L-glutamine; GIBCO, Thermo Fisher Scientific, USA) for 18 h before performing the LDH cytotoxicity assay using the LDH release kit (G1780 CytoTox 96; Promega) under the following conditions: E:T ratio of 5:1 (3×10^4 target cells/well and 1.5×10^5 CAR-T cells/well), E:T ratio of 8:1 (3×10^4 target cells/well and 2.4×10^5 CAR-T cells/well), and E:T ratio of 10:1 (3×10^4 target cells/well and 3×10^5 CAR-T cells/well).

Cytokine Release Assay

A multi-cytokine assay kit (560484; BD Biosciences, Franklin Lakes, NJ, USA) was used to measure the cytokine levels in supernatants from the coculture experiments (E:T ratio of 8:1) after CAR-T cell injection, according to the manufacturer's instructions.

Flow Cytometry

All four groups (NC, CAR-T-2598, CAR-T-1847, and CAR-T-1848) of cells (5×10^5/well) were seeded in 24-well plates and incubated with GolgiStop (00-4970-93; eBioscience, Thermo Fisher Scientific, USA) and Protein Transport Inhibitor Cocktail (00-4980-93; eBioscience,

Thermo Fisher Scientific, USA) for 5 h for CAR-T cell phenotype analysis. Cells were stained with the following fluorophore-conjugated monoclonal antibodies: MSLN (AARz0215081; R&D Systems, USA), biotin-protein L (RPL-PF141; ACROBiosystems, China), CD8 (344722; BioLegend, San Diego, CA, USA), IFNγ (12-7319-42; eBioscience, Thermo Fisher Scientific, USA), and TNF-α (25-7349-82; eBioscience, Thermo Fisher Scientific, USA). Next, the cells were fixed and permeabilized using eBioscience Fixation/Permeabilization reagent (00-5123-43; Invitrogen, Thermo Fisher Scientific, USA) and buffer (00-8333-56; Invitrogen) for flow cytometry using an Attune Cytometer (Thermo Fisher Scientific, USA). Data analysis was performed using FlowJo software, version 10.0 (BD Biosciences, USA).

Statistical Analysis

Statistical analysis was performed using GraphPad Prism software, version 7.00 (GraphPad Software, San Diego, CA, USA). Data from triplicate wells from at least three independent experiments were presented as the mean ± standard deviation. The Student's t test was used for comparison between two groups, and one-way analysis of variance and Tukey's post hoc tests were used to compare more than two groups. The p values <0.05 were deemed statistically significant (*$p < 0.05$; **$p < 0.01$; ***$p < 0.001$).

SUPPLEMENTAL INFORMATION

Supplemental Information can be found online at https://doi.org/10.1016/j.omto.2020.01.008.

AUTHOR CONTRIBUTIONS

L.Z., Y.L., F.Z., Y.J., and J.F. searched the literature. L.Z., L.Y., and Y.W. designed the experiments and wrote the paper. L.Z., R.G., and L.K. conducted the experiments, and collected and analyzed the data.

CONFLICTS OF INTEREST

The authors declare no competing interests.

ACKNOWLEDGMENTS

We would like to thank Prof. Lei Yu's group for providing technical support. We would like to acknowledge the Fund of the Translational Medical Center of HMU (grant no. 201809 to Y.W.); the National Natural Science Foundation of China (grant no. 81902421); the China Postdoctoral Science Foundation (grant no. 2018M641863); the Foundation of the Health Commission of Heilongjiang Province of China (grant no. 2018349); and a grant from the First Hospital of HMU (grant no. 2019B22) (to L.Z.) for funding this study.

REFERENCES

1. Siegel, R.L., Miller, K.D., and Jemal, A. (2019). Cancer statistics, 2019. CA Cancer J. Clin. *69*, 7–34.
2. Hidalgo, M. (2010). Pancreatic cancer. N. Engl. J. Med. *362*, 1605–1617.
3. Von Hoff, D.D., Ervin, T., Arena, F.P., Chiorean, E.G., Infante, J., Moore, M., Seay, T., Tjulandin, S.A., Ma, W.W., Saleh, M.N., et al. (2013). Increased survival in pancreatic cancer with nab-paclitaxel plus gemcitabine. N. Engl. J. Med. *369*, 1691–1703.
4. Conroy, T., Desseigne, F., Ychou, M., Bouché, O., Guimbaud, R., Bécouarn, Y., Adenis, A., Raoul, J.L., Gourgou-Bourgade, S., de la Fouchardière, C., et al.; Groupe Tumeurs Digestives of Unicancer; PRODIGE Intergroup (2011). FOLFIRINOX versus gemcitabine for metastatic pancreatic cancer. N. Engl. J. Med. *364*, 1817–1825.
5. Maude, S.L., Frey, N., Shaw, P.A., Aplenc, R., Barrett, D.M., Bunin, N.J., Chew, A., Gonzalez, V.E., Zheng, Z., Lacey, S.F., et al. (2014). Chimeric antigen receptor T cells for sustained remissions in leukemia. N. Engl. J. Med. *371*, 1507–1517.
6. Grupp, S.A., Kalos, M., Barrett, D., Aplenc, R., Porter, D.L., Rheingold, S.R., Teachey, D.T., Chew, A., Hauck, B., Wright, J.F., et al. (2013). Chimeric antigen receptor-modified T cells for acute lymphoid leukemia. N. Engl. J. Med. *368*, 1509–1518.
7. Hinrichs, C.S., and Restifo, N.P. (2013). Reassessing target antigens for adoptive T-cell therapy. Nat. Biotechnol. *31*, 999–1008.
8. Maus, M.V., Haas, A.R., Beatty, G.L., Albelda, S.M., Levine, B.L., Liu, X., Zhao, Y., Kalos, M., and June, C.H. (2013). T cells expressing chimeric antigen receptors can cause anaphylaxis in humans. Cancer Immunol. Res. *1*, 26–31.
9. Ene-Obong, A., Clear, A.J., Watt, J., Wang, J., Fatah, R., Riches, J.C., Marshall, J.F., Chin-Aleong, J., Chelala, C., Gribben, J.G., et al. (2013). Activated pancreatic stellate cells sequester CD8+ T cells to reduce their infiltration of the juxtatumoral compartment of pancreatic ductal adenocarcinoma. Gastroenterology *145*, 1121–1132.
10. Beatty, G.L., O'Hara, M.H., Lacey, S.F., Torigian, D.A., Nazimuddin, F., Chen, F., Kulikovskaya, I.M., Soulen, M.C., McGarvey, M., Nelson, A.M., et al. (2018). Activity of Mesothelin-Specific Chimeric Antigen Receptor T Cells Against Pancreatic Carcinoma Metastases in a Phase 1 Trial. Gastroenterology *155*, 29–32.
11. Zhao, L., Li, J., Liu, Y., Kang, L., Chen, H., Jin, Y., Zhao, F., Feng, J., Fang, C., Zhu, B., et al. (2018). Cholesterol Esterification Enzyme Inhibition Enhances Antitumor Effects of Human Chimeric Antigen Receptors Modified T Cells. J. Immunother. *41*, 45–52.
12. Chang, T.Y., Li, B.L., Chang, C.C., and Urano, Y. (2009). Acyl-coenzyme A:cholesterol acyltransferases. Am. J. Physiol. Endocrinol. Metab. *297*, E1–E9.
13. Brown, M.S., and Goldstein, J.L. (1983). Lipoprotein metabolism in the macrophage: implications for cholesterol deposition in atherosclerosis. Annu. Rev. Biochem. *52*, 223–261.
14. Yang, W., Bai, Y., Xiong, Y., Zhang, J., Chen, S., Zheng, X., Meng, X., Li, L., Wang, J., Xu, C., et al. (2016). Potentiating the antitumour response of CD8(+) T cells by modulating cholesterol metabolism. Nature *531*, 651–655.
15. Lochner, M., Berod, L., and Sparwasser, T. (2015). Fatty acid metabolism in the regulation of T cell function. Trends Immunol. *36*, 81–91.
16. Johnston, F.M., Tan, M.C.B., Tan, B.R., Jr., Porembka, M.R., Brunt, E.M., Linehan, D.C., Simon, P.O., Jr., Plambeck-Suess, S., Eberlein, T.J., Hellstrom, K.E., et al. (2009). Circulating mesothelin protein and cellular antimesothelin immunity in patients with pancreatic cancer. Clin. Cancer Res. *15*, 6511–6518.
17. Morello, A., Sadelain, M., and Adusumilli, P.S. (2016). Mesothelin-Targeted CARs: Driving T Cells to Solid Tumors. Cancer Discov. *6*, 133–146.
18. Levine, B.L., Humeau, L.M., Boyer, J., MacGregor, R.R., Rebello, T., Lu, X., Binder, G.K., Slepushkin, V., Lemiale, F., Mascola, J.R., et al. (2006). Gene transfer in humans using a conditionally replicating lentiviral vector. Proc. Natl. Acad. Sci. USA *103*, 17372–17377.
19. Lim, W.A., and June, C.H. (2017). The Principles of Engineering Immune Cells to Treat Cancer. Cell *168*, 724–740.
20. Hassan, R., Kindler, H.L., Jahan, T., Bazhenova, L., Reck, M., Thomas, A., Pastan, I., Parno, J., O'Shannessy, D.J., Fatato, P., et al. (2014). Phase II clinical trial of amatuximab, a chimeric antimesothelin antibody with pemetrexed and cisplatin in advanced unresectable pleural mesothelioma. Clin. Cancer Res. *20*, 5927–5936.
21. Beatty, G.L., Haas, A.R., Maus, M.V., Torigian, D.A., Soulen, M.C., Plesa, G., Chew, A., Zhao, Y., Levine, B.L., Albelda, S.M., et al. (2014). Mesothelin-specific chimeric antigen receptor mRNA-engineered T cells induce anti-tumor activity in solid malignancies. Cancer Immunol. Res. *2*, 112–120.
22. Long, K.B., Gladney, W.L., Tooker, G.M., Graham, K., Fraietta, J.A., and Beatty, G.L. (2016). IFNγ and CCL2 Cooperate to Redirect Tumor-Infiltrating Monocytes to

Degrade Fibrosis and Enhance Chemotherapy Efficacy in Pancreatic Carcinoma. Cancer Discov. *6*, 400–413.

23. Roybal, K.T., Rupp, L.J., Morsut, L., Walker, W.J., McNally, K.A., Park, J.S., and Lim, W.A. (2016). Precision Tumor Recognition by T Cells With Combinatorial Antigen-Sensing Circuits. Cell *164*, 770–779.

24. Winograd, R., Byrne, K.T., Evans, R.A., Odorizzi, P.M., Meyer, A.R., Bajor, D.L., Clendenin, C., Stanger, B.Z., Furth, E.E., Wherry, E.J., and Vonderheide, R.H. (2015). Induction of T-cell Immunity Overcomes Complete Resistance to PD-1 and CTLA-4 Blockade and Improves Survival in Pancreatic Carcinoma. Cancer Immunol. Res. *3*, 399–411.

25. Shi, X., Bi, Y., Yang, W., Guo, X., Jiang, Y., Wan, C., Li, L., Bai, Y., Guo, J., Wang, Y., et al. (2013). Ca2+ regulates T-cell receptor activation by modulating the charge property of lipids. Nature *493*, 111–115.

26. Swamy, M., Beck-Garcia, K., Beck-Garcia, E., Hartl, F.A., Morath, A., Yousefi, O.S., Dopfer, E.P., Molnár, E., Schulze, A.K., Blanco, R., et al. (2016). A Cholesterol-Based Allostery Model of T Cell Receptor Phosphorylation. Immunity *44*, 1091–1101.

27. Prantner, A.M., Yin, C., Kamat, K., Sharma, K., Lowenthal, A.C., Madrid, P.B., and Scholler, N. (2018). Molecular Imaging of Mesothelin-Expressing Ovarian Cancer with a Human and Mouse Cross-Reactive Nanobody. Mol. Pharm. *15*, 1403–1411.

28. Carpenito, C., Milone, M.C., Hassan, R., Simonet, J.C., Lakhal, M., Suhoski, M.M., Varela-Rohena, A., Haines, K.M., Heitjan, D.F., Albelda, S.M., et al. (2009). Control of large, established tumor xenografts with genetically retargeted human T cells containing CD28 and CD137 domains. Proc. Natl. Acad. Sci. USA *106*, 3360–3365.

OMTO, Volume *16*

Supplemental Information

Inhibition of Cholesterol Esterification Enzyme Enhances the Potency of Human Chimeric Antigen Receptor T Cells against Pancreatic Carcinoma

Lei Zhao, Yang Liu, Fuya Zhao, Ye Jin, Jing Feng, Rui Geng, Jiayu Sun, Liqing Kang, Lei Yu, and Yunwei Wei

Supplementary Figure S1. The cytokine release in all MSLN-negative target groups after standard LDH release assays.

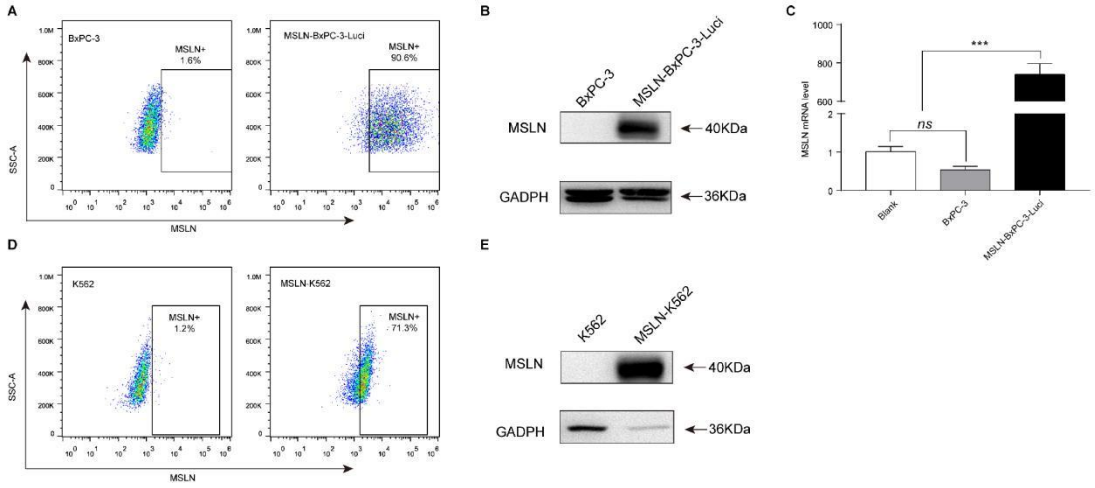

Supplementary Figure S2. Immunofluorescence image showing MSLN expression in mouse PC tissue. MSLN-positive cell membrane, red; cell nucleus, blue.

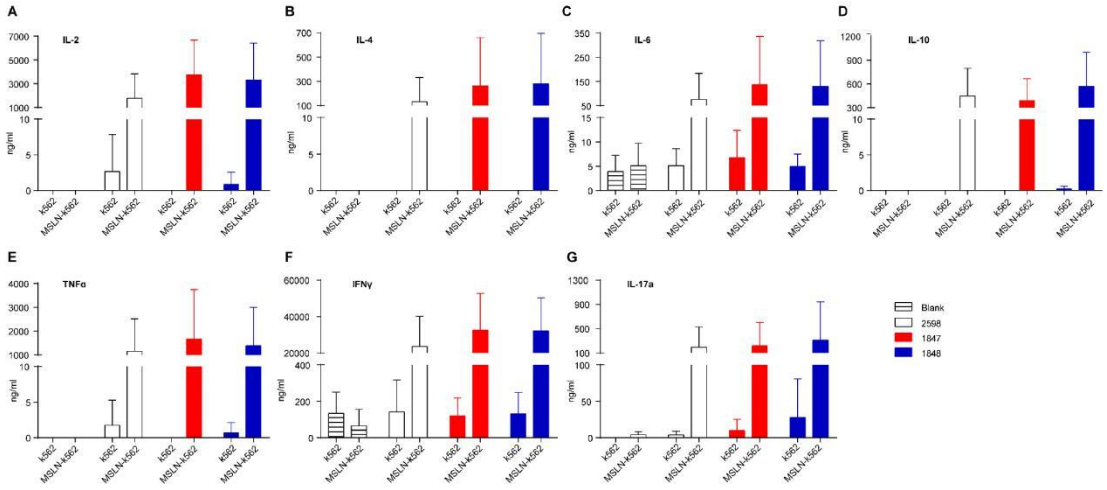

Supplementary Figure S3. Immunofluorescence image showing targeting MSLN CAR-T cell infiltration in mouse PC tissue. MSLN-positive cell membrane, red; cell nucleus, blue. Representative targeting MSLN CAR-T cells in OC tissue are indicated by the yellow arrow.

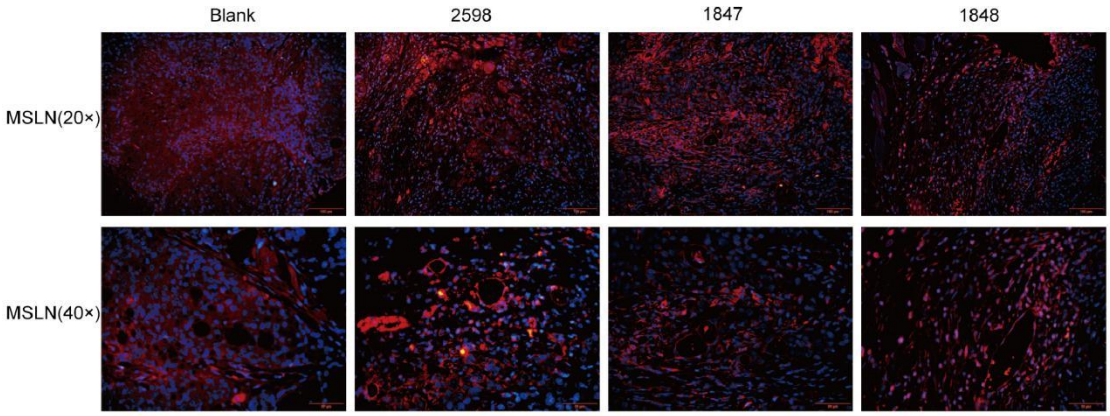

Supplementary Figure S4. Detection of MSLN expression in target cells. MSLN expression levels in BxPC-3 and MSLN-BxPC-3-Luci cells as determined using (A) flow cytometry, (B) western blotting, and (C) quantitative real-time RT-PCR. (D) Flow cytometry profile and (E) western blot image showing MSLN expression in K562 cells and MSLN-K562 cells.

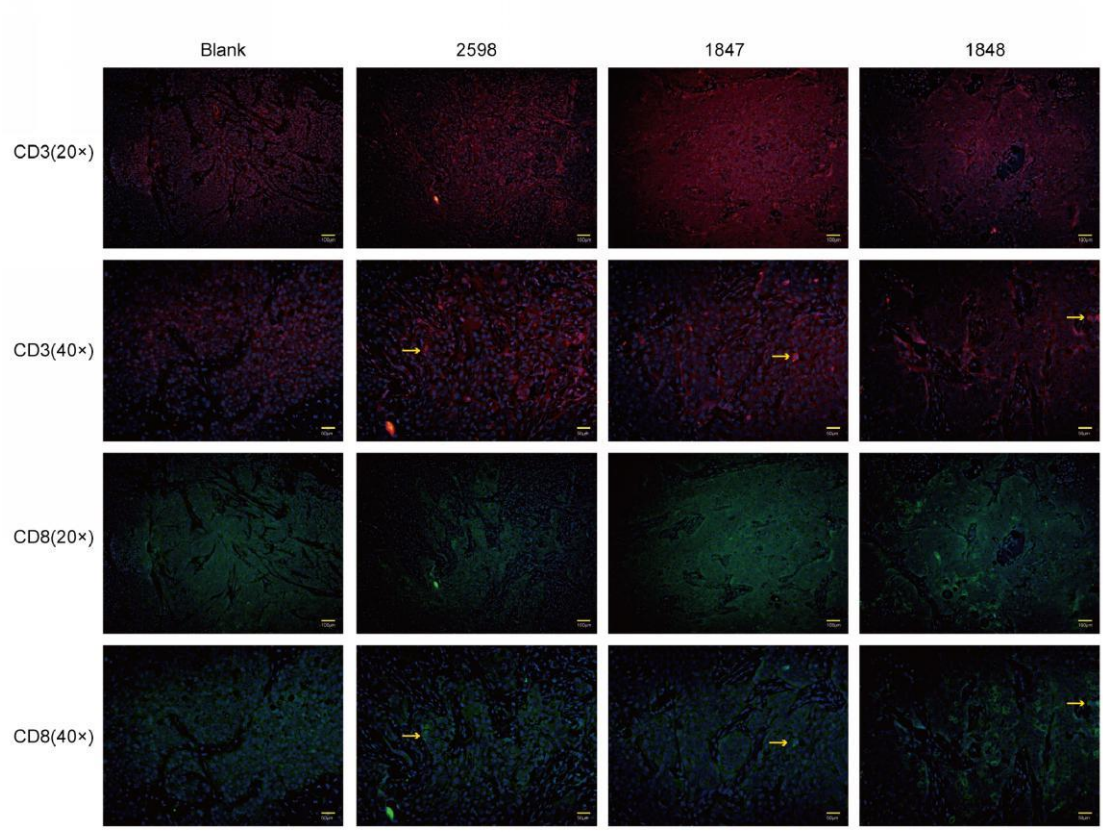

Supplementary Table S1. Profile showing the CAR transduction efficiency of targeting MSLN CAR-T cells.

	CAR-T-2598	CAR-T-1847	CAR-T-1848
Case 1	75.97%	71.20%	66.23%
Case 2	70.13%	70.53%	58.73%
Case 3	65.17%	58.43%	54.57%
Case 4	21.93%	12.63%	14.87%
Case 5	20.23%	13.97%	14.63%
Case 6	30.30%	18.30%	13.40%

Supplementary Table S2. Patient and healthy control group information.

	Normal (n = 5)	[a]AP (n = 6)	[b]PC (n = 9)	[c]M-PC (n = 4)
Gender				
female	0	3	2	0
male	5	3	7	4
Age(mean±SE)	28.2±1.2	58.3±11.3	64.0±9.7	56.8±3.9

[a]AP: Acute Pancreatitis; [b]PC: Pancreatic Cancer; [c]M-PC: Pancreatic Cancer with Metastasis